Dynamic Characteristics of HDD Slider by Perturbated Direct Numerical Method

Polina V. Khan* and Pyung Hwang**

*Graduate student, Department of Mechanical Engineering, Yeungnam University

** School of Mechanical Engineering, Yeungnam University, Korea

214-1 Dae-Dong, Gyongsan, Gyongbuk 712-749 KOREA

The static and dynamic characteristics of HDD slider with ulta-low flying height are analyzed using Direct Numerical method with Boundary Fitted Coordinate System. The slip flow effect is considered using the Boltzmann equation solution in a form of the flow rate database. The air film stiffness and damping are evaluated by the small perturbation method.

Keywords: Air Bearing, Direct Numerical, Small Perturbation, Hard Disk Drive Slider

Introduction

One of the main directions in the development of computer technology is increasing hard disk capacity. The reading/writing elements, mounted at the hard disk head, should be positioned close to the disk surface to work with high-density data.

Prediction of the air bearing forces and moments requires solution of the Reynolds equation, which describes the pressure distribution in the air film between head (slider) and disk. One of the numerical methods, which can deal with complicated boundary conditions, is the Boundary Fitted Coordinate System (BFCS) Direct Numerical method [1].

For the sliders with flying heights below 0.1 μm the slip flow effect should be considered. Fukui and Kaneko [2] proposed a database of the flow rate coefficients for the generalized Reynolds equation applicable in a wide range of Knudsen number values.

The stiffness and damping properties of the air film can be obtained by the use of the small perturbation method [3], [4].

In the present work the dynamic characteristics of the femto-slider are researched by perturbated BFCS Direct Numerical method, with application of the flow rate database.

Fundamental equations

The isothermal generalized Reynolds equation is equivalent to the mass conservation law

$$\frac{\partial q^x}{\partial x} + \frac{\partial q^y}{\partial y} + \frac{\partial q^z}{\partial z} = 0 \qquad (1)$$

where

$$q^x = -\frac{h^2 Q_P}{2D_0\mu}\frac{\partial p}{\partial x} + \frac{Uph}{2}$$
$$q^y = -\frac{h^2 Q_P}{2D_0\mu}\frac{\partial p}{\partial y} + \frac{Vph}{2} \qquad (2)$$
$$\frac{\partial q^z}{\partial z} = \frac{\partial (ph)}{\partial t}$$

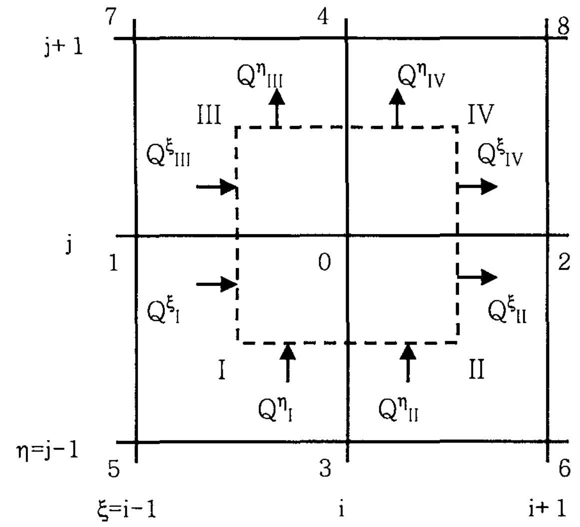

Figure 1. Total flow into the control volume

Q_P is the Poiseuille flow rate coefficient [2]. $D=D_0\,p\,h$ is the inverse Knudsen number.

In order to accurately describe the boundary conditions the mesh in the physical domain (x,y) is drawn so that the mesh lines follows the film thickness steps boundaries. Such mesh is called the Boundary-Fitted Coordinate System (BFCS). In the computational domain (ξ, η) the mesh is rectilinear with equidistant nodes position.

In the static analysis the term with time derivative is omitted and the mass fluxes in the computational domain are given by

$$Q^{\xi} \underset{\xi=\xi_0}{=} \int_{\eta_1}^{\eta_2} \left(-Ap_{\xi} + Bp_{\eta} + Dp\right) d\eta$$
$$Q^{\eta} \underset{\eta=\eta_0}{=} \int_{\xi_1}^{\xi_2} \left(Bp_{\xi} - Cp_{\eta} + Ep\right) d\xi \qquad (3)$$

where A, B, C, D and E are defined as

$$\begin{aligned}
\alpha &= x_{\eta}^2 + y_{\eta}^2 \\
\beta &= x_{\eta}x_{\xi} + y_{\eta}y_{\xi} \\
\gamma &= x_{\xi}^2 + y_{\xi}^2 \\
J &= x_{\xi}y_{\eta} - x_{\eta}y_{\xi} \\
A &= h^2 Q_P \alpha / (2\mu J D_0) \\
B &= h^2 Q_P \beta / (2\mu J D_0) \\
C &= h^2 Q_P \gamma / (2\mu J D_0) \\
D &= h\left(y_{\eta}U - x_{\eta}V\right) \\
E &= h\left(-y_{\xi}U + x_{\xi}V\right)
\end{aligned} \qquad (4)$$

Consider small oscillations of the slider with corresponding perturbations of the air film thickness, pressure distribution and Poiseuille flow rate coefficient

$$\begin{aligned}
h &= \overline{h} + \varepsilon \hat{h} e^{j\nu t} \\
p &= \overline{p} + \varepsilon \hat{p} e^{j\nu t} \\
Q_P &= \overline{Q}_P + \varepsilon \frac{\partial Q_P}{\partial D} D_0 \left(\overline{p}\hat{h} + \hat{p}\overline{h}\right) e^{j\nu t}
\end{aligned} \qquad (5)$$

where $\overline{h}$ and $\overline{p}$ denotes the values at the steady state, j is the imaginary unit and ε and ν are the perturbation amplitude and frequency correspondingly.

When substituted to Equations (3, 4) it gives the following expressions for the perturbed mass flux

$$\hat{Q}^{\xi} \underset{\xi=\xi_0}{=} \int_{\eta_1}^{\eta_2} \left(-\overline{A}\hat{p}_{\xi} + \overline{B}\hat{p}_{\eta} + \overline{D}\hat{p} + \hat{F}\right) d\eta$$
$$\hat{Q}^{\eta} \underset{\eta=\eta_0}{=} \int_{\xi_1}^{\xi_2} \left(\overline{B}\hat{p}_{\xi} - \overline{C}\hat{p}_{\eta} + \overline{E}\hat{p} + \hat{G}\right) d\xi \qquad (6)$$

where the coefficients of perturbed pressure derivatives are

$$\overline{A} = \overline{h}^2\overline{Q}_P\alpha/(2\mu JD_0)$$
$$\overline{B} = \overline{h}^2\overline{Q}_P\beta/(2\mu JD_0) \quad (7)$$
$$\overline{C} = \overline{h}^2\overline{Q}_P\gamma/(2\mu JD_0)$$

the coefficients of perturbed pressure are

$$\overline{D} = \overline{h}(y_\eta U - x_\eta V) + \frac{\partial Q_P}{\partial D}\frac{\overline{h}^3}{2\mu J}(-\alpha\overline{p}_\xi + \beta\overline{p}_\eta) \quad (8)$$
$$\overline{E} = \overline{h}(-y_\xi U + x_\xi V) + \frac{\partial Q_P}{\partial D}\frac{\overline{h}^3}{2\mu J}(\beta\overline{p}_\xi - \gamma\overline{p}_\eta)$$

and the absolute terms are

$$\hat{F} = \hat{h}\left(2\overline{h}\,\overline{Q}_P + \overline{h}^2\frac{\partial Q_P}{\partial D}D_0\overline{p}\right)\frac{(-\alpha\overline{p}_\xi + \beta\overline{p}_\eta)}{2\mu D_0 J} + \hat{h}\overline{p}(Uy_\eta - Vx_\eta) \quad (9)$$
$$\hat{G} = \hat{h}\left(2\overline{h}\,\overline{Q}_P + \overline{h}^2\frac{\partial Q_P}{\partial D}D_0\overline{p}\right)\frac{(+\beta\overline{p}_\xi - \gamma\overline{p}_\eta)}{2\mu D_0 J} + \hat{h}\overline{p}(-Uy_\xi + Vx_\xi)$$

The approximate values of $\partial Q_P/\partial D$ are obtained from the database, using the finite differences.

The squeeze film flow appears as z-component of the perturbed mass flux

$$\hat{Q}^z = jv\iint(\hat{h}\overline{p} + \overline{h}\hat{p})Jd\xi d\eta \quad (10)$$

The control volume, used in the Direct Numerical method with BFCS, includes nine nodes and the total mass flux is calculated separately in the four zones around the central node (Fig. 1) [1].

Sliders characteristics

The slider's position is described by flying height h_f, pitching angle ϕ, and rolling angle θ

$$\vec{S} = \{h_f, \phi, \theta\} \quad (11)$$

The air bearing lifting force, and it's moment about the mass center are calculated as follows

$$L = \iint p(x,y)dxdy$$
$$M_\phi = \iint p(x,y)(x - x_c)dxdy \quad (12)$$
$$M_\theta = \iint p(x,y)(y - y_c)dxdy$$

The steady state position is defined from the force and moments balance by multidimensional Newton-Raphson method, combined with optimization scheme [5].

The film thickness perturbation is a combination of small displacements in vertical, pitching and rolling directions

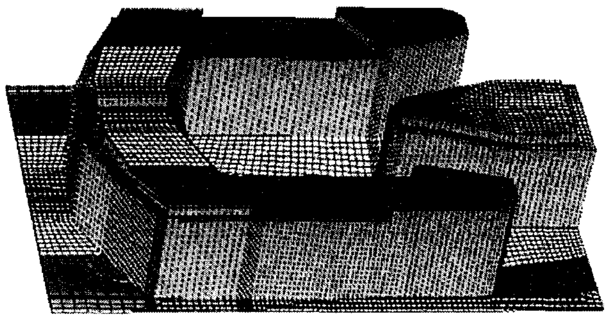

Figure 2. Five-pad negative pressure slider

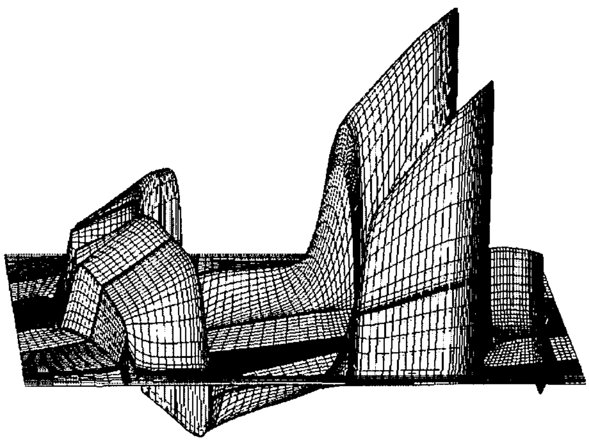

Figure 3. Pressure distribution

$$\hat{h}(x,y) = \hat{h}_f + \hat{\phi}(x - x_c) + \hat{\theta}(y - y_c) \quad (13)$$

The perturbed pressure corresponding to unit displacements is denoted by G_i - complex stiffness, which can be determined from the perturbed flux balance (Eq. 6)

$$\hat{p} = G_1 \hat{h}_f + G_2 \hat{\phi} + G_3 \hat{\theta} = \sum G_i \hat{s}_i \quad (14)$$

The air film stiffness and damping matrixes are expressed as follows [3, 4]

$$K_{1,j} = \frac{\partial L}{\partial s_j} = \iint \Re(G_j) dxdy$$
$$K_{2,j} = \frac{\partial M_\phi}{\partial s_j} = \iint \Re(G_j)(x - x_c) dxdy \quad (15)$$
$$K_{3,j} = \frac{\partial M_\theta}{\partial s_j} = \iint \Re(G_j)(y - y_c) dxdy$$

$$C_{1,j} = \frac{\partial L}{\partial \dot{s}_j} = \frac{1}{jv} \iint \Im(G_j) dxdy$$
$$C_{2,j} = \frac{\partial M_\phi}{\partial \dot{s}_j} = \frac{1}{jv} \iint \Im(G_j)(x - x_c) dxdy \quad (16)$$
$$C_{3,j} = \frac{\partial M_\theta}{\partial \dot{s}_j} = \frac{1}{jv} \iint \Im(G_j)(y - y_c) dxdy$$

Computational results

Five-pad negative pressure (NP) femto-slider (Fig. 2) is one designed for modern HDD with 1Tb/in^2 storage density. Sub-ambient pressure in the central cavity pull slider close to disk while high pressure at the pads supports the slider (Fig. 3).

Parameters of slider-disk interface are given in the Table 1. The steady state position were determined for 0.5 gf preload at the slider's center.

Table 1. Slider's parameters

Length, b (mm)	0.82
Width, l (mm)	0.66
Base recess (nm)	2500
Shallow recess (nm)	300
Crown (nm)	18
Camber (nm)	2
Skew angle	0
Disk speed (rpm)	7200

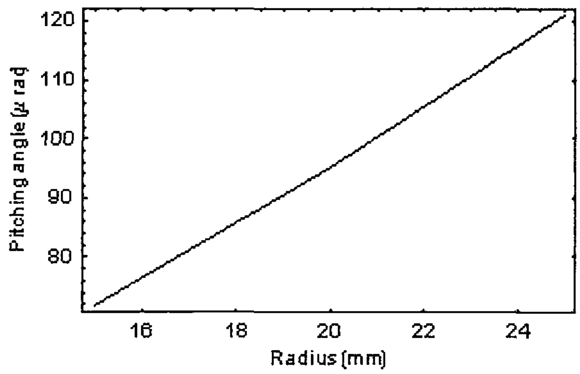

Figure 4. Pitching angle at steady state position

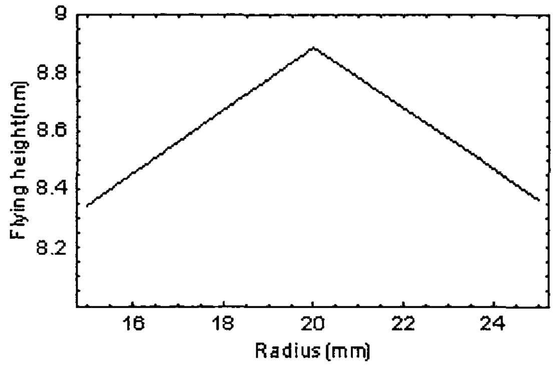

Figure 5. Flying height at steady state position

Due to significant crown the highest pressure is generated not at the trailing edge but at the rails pads. The disk surface velocity increases with the slider's radial position and it can be expected that the slider will fly higher at the outer radius. In the

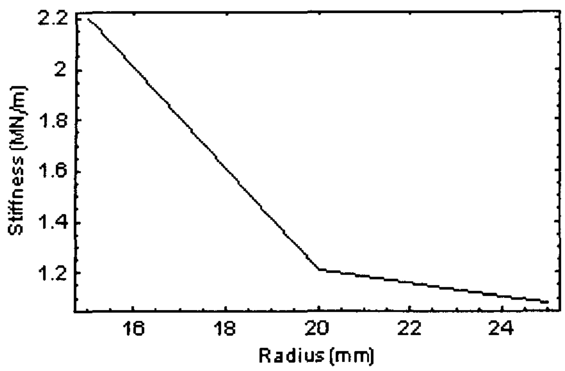

Figure 6. Stiffness for vertical vibrations

present case the force balance at the bigger radius is achieved by increasing the pitching angle (Fig. 4) almost without changing the flying height at the trailing edge (Fig. 5). The stiffness for vertical oscillations (Fig. 6) decreases with increasing radius, because the air film thickness at the rails increases and the total upward force remains equal to preload.

Conclusions

The BFCS Direct numerical method is adapted to analysis of sliders with high Knudsen number by using the flow rate database. The static and dynamic properties of the five-pad NP femto slider under 0.5 gf preload were investigated, considering different radial position of slider. The flying height at the steady state is about 8 nm and does not change with sliders radial position. The pitch angle increases linearly from 70 μrad at the inner radius to 120 μrad at the outer radius. The stiffness decreases from 2.2MN/m at inner radius to 1.1 MN/m at the outer radius.

Nomenclature

p: pressure

h: air film thickness

U,V: disk velocity components

μ: air viscosity

References

1. Kawabata N., "A Useful Numerical Analysis Method for the Dynamic Characteristics of Fluid Film Lubrication (The case of Incompressible Fluid Lubrication)," JSME Int. Journal, 34(1), 1991, 91-96.
2. Fukui S., and Kaneko R., "A Database for Interpolation of Poiseuille Flow Rates for High Knudsen number lubrication Problems," ASME J. of Tribology, Vol.112, pp. 78-83, 1990
3. Ono K., "Dynamic Characteristics of Air-Lubricated Slider Bearing for Noncontact Magnetic Recording," ASME Journal of Lubrication Technology, 97, 1975, 250-260.
4. Hwang P., Park S.S. and Kim E., "A Study on Lubricative Characteristics of the Negative Pressure Slider," KSTLE Int. Journal, Vol. 3, No. 2, 2002, 110-113
5. Hwang P. and Khan P., "Direct Numerical Analysis of Slider Using Optimization Scheme," 2003, Proceedings of IASTED (MIC).